Biophysical Journal, Volume *110*

Supplemental Information

Untangling the Influence of a Protein Knot on Folding

Dominique T. Capraro and Patricia A. Jennings

Supporting Text

We collected and analyzed unfolding and refolding kinetic data with manual mixing techniques and circular dichroism (CD) spectroscopy. We followed the time-dependent change in signal at 222 nm to follow the changes in secondary structure(s) as a function of time at each denaturant concentration in this topologically-challenged folding reaction. Experiments were conducted monitoring the signal change upon dilution into varying concentrations of denaturant, of native protein (unfolding), as well as diluting protein incubated in 6M Gnd-HCl, for the times indicated, into conditions favoring the refolding of the protein (refolding jump), yielding traces that reached completion on a timescale of tens' of seconds (Fig. S1).

The acquired data were analyzed and fit to both a single and double exponential equation, in order to determine the kinetic rate constants associated with the associated folding/unfolding reactions. Similar to previous experimental folding studies on a knotted protein (23), we fit the folding data to a single rate exponential, however as with the previous study, a single exponential fit is inadequate. A bi-exponential fit of the observed kinetic reactions, based on assessment of the residuals (Fig. SB), best describes the data. A plot of the natural log of the rate constants, both single (Fig. S2, green) and double (Fig. S2, blue, purple) as a function of denaturant revealed folding arms that are not typically observed in a chevron analysis (Fig. S2). Interestingly, both data sets reveal an unusual trend, where the rate constants in both refolding and unfolding are not completely linearly-dependent on the denaturant concentration (Fig. S2). For the signle exponential fits, this phase is the dominant signal. In addition, for the bi-exponential fit, one phase displays typical increase in rate at lower denaturant concentrations upon refolding while the subsequent phase displays decreasing rates as a function of decreasing denaturant concentration upon initiation of the refolding reaction. Likewise, upon increasing denaturant concentration in unfolding conditions one phase increases with denaturant concentration, as expected for folding, until it plateaus, while the slower phase is independent of denaturant concentration. This non-protein-folding-like behavior seen in the slower phase, referred to as an inverted chevron, we associate with the complex topology of the knot. More specifically, the inverted folding behavior in the refolded arm (Fig. SI2, green), and the severe rollover in the unfolding arm, suggest that the folding reaction is far more complex than a typical folding analysis can characterize. We attribute these unique trends with the presence of the knot topology and the tying/untying reaction. Furthermore, the comparative analyses of the varied exponential fits (Fig. S2, green versus purple) reveal that the observed signal associated with the mechanism of knotting dominates the folding landscape.

Supporting Figure Legends:

Fig. S1: Sample kinetic traces from the manual mixing kinetics of MTT_{Tm}.
(A) Kinetic traces of the manual mixing unfolding (4.8M, blue) and refolding (3.2M, green) experiments monitoring the change in ellipticity at 222nm. The lines reflect the biphasic exponential fit. (B) Residuals for the mono-exponential (left) and bi-exponential (right) fits of the CD refolding kinetic data at the 3.0M dilution.

Fig. S2: Chevron plot of the kinetic fits of the acquired optical data.
Mono- (green circles) and bi-exponential (blue and purple lines) fits of the manual mixing kinetic traces reveal a unique inverted rate behavior, attributed to the formation of the knot. The black dotted lines guide the curve, representing an ideal fit, where rollover in either arm is not observed.

Fig. S3: Determination of the stability of the knot.
(A) Using the kinetic constants determined, equilibrium curves were generated for the protein (black) and the knot (purple). These curves were fit similarly to the denaturant-dependent curves (dashed lines). (B) The thermodynamic values for the knot generated by the fitting.

Supporting Figures:

Fig. S1

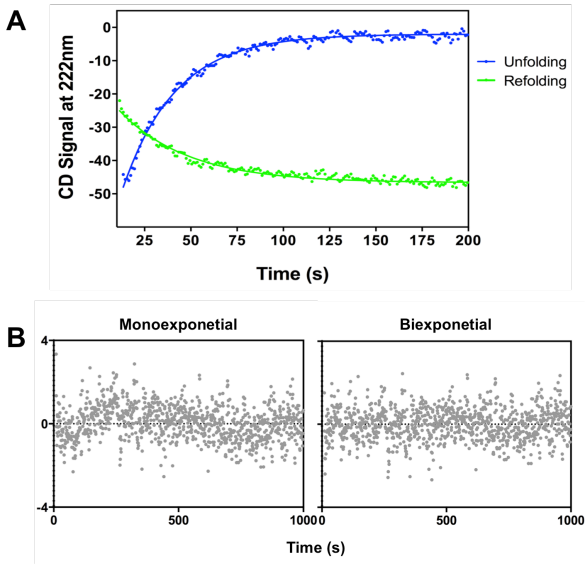

Fig. S2

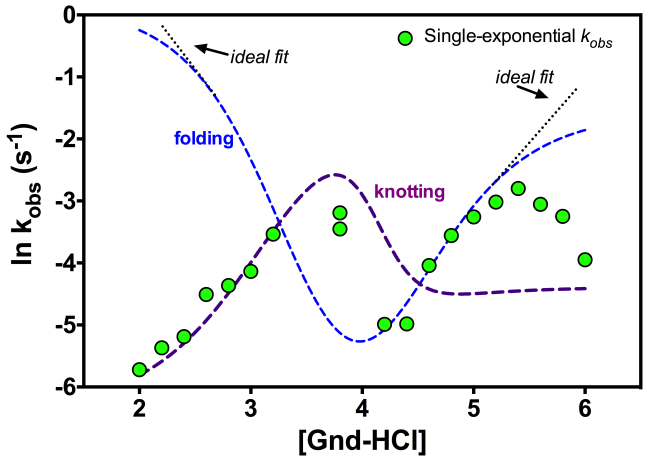

Fig. S3

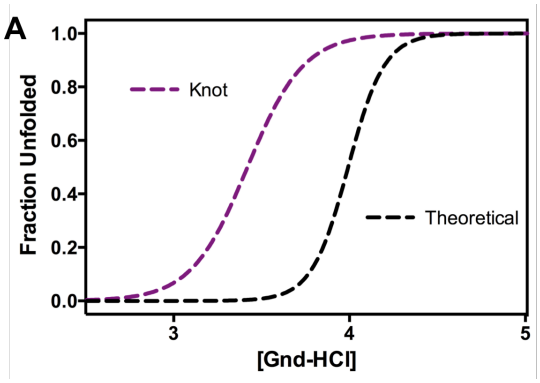

B

	$\Delta G_{N\text{-}U}$[a,b] (kcalmol^{-1})	$\Delta\Delta G_{N\text{-}U}$[a,b] (kcalmol^{-1})	*m*-value$_{N\text{-}U}$[a,b] (kcalmol^{-1}M^{-1})	C_m[c] (M)
Knot	12.7±0.1	-8.4±0.2	3.7±0.1	3.4

The theoretical equilibrium data were fit using GraphPad Prism 6 in order to obtain equilibrium parameters for folding, $\Delta G_{N\text{-}U}$. Changes in $\Delta G_{N\text{-}U}$ ($\Delta\Delta G_{N\text{-}U}$) were obtained using unfolding as a reference. *m*-value indicates changes in the accessible surface area upon folding and indicate cooperativity of folding.
[a] Equilibrium transition data were evaluated using a two-state folding model.
[b] Data were obtained by calculating the Fapp as a function of [Gnd-HCl] at 222nm via CD, based on rates of folding.
[c] C_m values were taken from dividing the $\Delta G_{N\text{-}U}$ by the *m*-value.